DOI: 10.1002/ejic.200600902

Synthesis, Crystal Structures, and Oxidation States of MM′X-Type Platinum–Rhodium Dinuclear Complexes Having Amidate Bridging Ligands

Kazuhiro Uemura,[a][‡] Kana Yamasaki,[a] Kôichi Fukui,[a][‡‡] and Kazuko Matsumoto*[a][‡‡‡]

Keywords: Platinum / Rhodium / 1D Chains / Dinuclear complexes

Six novel Pt–Rh dinuclear complexes (**1**–**6**), $[PtRh(PVM)_2(NH_3)_2Cl_3]\cdot 4H_2O$ (**1**, PVM = *t*BuCONH$^-$), $[PtRh(PVM)_2(en)Cl_3]\cdot 3H_2O$ (**2**, en = ethylenediamine), $[PtRh(PVM)_2(NH_2CH_3)_2Cl_3]\cdot 3H_2O$ (**3**), $[PtRh(PVM)_2(NH_2tBu)_2Cl_3]\cdot 3H_2O$ (**4**), $[PtRh(TCM)_2(NH_3)_2Cl_3]$ (**5**, TCM = Cl_3CCONH^-), and $[PtRh(BZM)_2(NH_3)_2Cl_3]\cdot H_2O$ (**6**, BZM = PhCONH$^-$), have been synthesized from Pt mononuclear complexes having nitrogen-coordinated amidate ligands with noncoordinated amidate oxygen atoms. X-ray analysis revealed that compounds **1** and **2** form zigzag one-dimensional chains in the form $[–Pt–Rh–Cl–]_n$. The oxidation states of the metal ions have been determined by X-ray photoelectron spectroscopy (XPS) and ^{195}Pt NMR spectroscopic analysis, and are Pt(+2, d^8)···Rh(+3, d^6). In comparison with the Pt–Rh distances found in the literature, it has become apparent that the Pt–Rh dinuclear complexes have a dative Pt(d^8)→Rh(d^6) bond, where the Pt d_{z^2} orbital is stabilized by the overlap with the d_{z^2} orbital of the Rh atom.

Introduction

One-dimensional (1D) metal complexes have been one of the intriguing subjects for the last several decades owing to their unusual electrical properties that are based on a variety of possible metal oxidation states.[1] Most of the 1D chains are made up of Rh(+1/+2) and/or Pt(+2/+3) because partial oxidation or reduction of the d_{z^2} orbital attributed to the $d^8 \leftrightarrow d^7$ redox change affords partially filled valence bands. Several 1D metal complexes comprising infinite –Pt–Pt– bonds[2] or –Rh–Rh– bonds[3] and halogen-bridged Pt (MX and MMX) chains[4,5] have been synthesized and investigated to present. MMX chains have mixed-valence states of the dinuclear units and adopt a variety of electronic structures represented by the four extreme valence-ordering states.[4] Control of the electronic structures by tailoring the ligands with subtle chemical modifications has been attempted with MMX chains.[4] However, control of the electronic structures by introduction of another metal (M′) to the MMX chains to make so-called MM′X chains has not been reported, to the best of our knowledge (Scheme 1). A series of MM′X chains is considered to be a new class of 1D metal complexes and is expected to have interesting electrical properties.

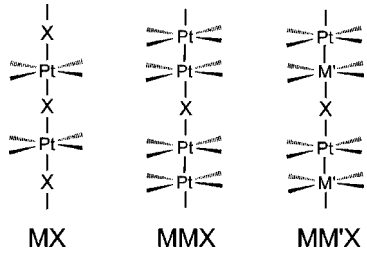

Scheme 1.

On the basis of the background above, we have tried to synthesize MM′X chains by starting with Pt mononuclear complexes with amidate ligands such as $[Pt(PVM)_2(NH_3)_2]\cdot 2H_2O$ (PVM = *t*BuCONH$^-$),[6] which can easily bind a second metal ion with the noncoordinated oxygen atoms in the amide moieties and afford various dinuclear and trinuclear Pt complexes (Scheme 2).[7] When M′ is one of the first transition metals (e.g. Co, Ni, Cu), trinuclear Pt–M′–Pt complexes are obtained because of their thermal stabilities and the ease of substitution of the ligands, even if the mixing ratio is 1:1 (Pt:M′).[6] Considering the undesired trimerization and the necessity of mixed valency for 1D chains, we selected Rh atoms as M′. Herein, we show the synthesis, crystallographic characterization, and determination of the formal metal oxidation states in Cl$^-$ ion bridged Pt–Rh dinuclear complexes.

[a] Department of Chemistry, Graduate School of Science and Engineering, Waseda University,
3-4-1, Ohkubo, Shinjuku, Tokyo 169-8555, Japan
Fax: +81-3-3413-5352
E-mail: kmatsu@yf6.so-net.ne.jp
[‡] Current address: Environmental Science and Engineering, Graduate School of Science and Engineering, Yamaguchi University,
Tokiwadai 2-16-1, Ube-shi, Yamaguchi, 755-8611, Japan
[‡‡] Current address: Graduate School of Life Science and Systems Engineering, Kyushu Institute of Technology,
Hibikino 2-4, Wakamatsu-ku, Kitakyushu 808-0196, Japan
[‡‡‡] Current address: 3-9-12-105, Daizawa,
Setagaya-ku, Tokyo 155-0032, Japan
Supporting information for this article is available on the WWW under http://www.eurjic.org or from the author.

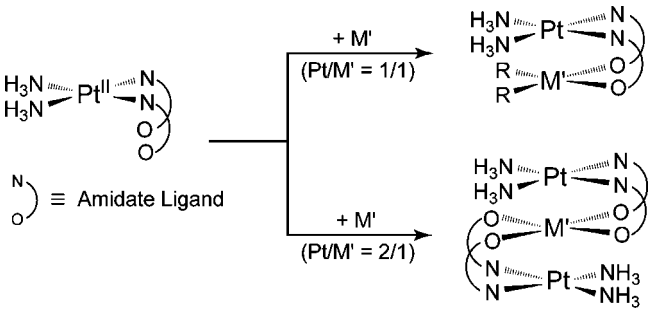

Scheme 2.

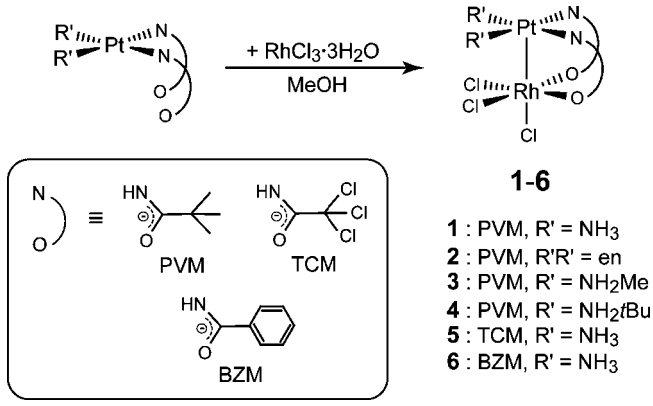

Scheme 3.

Results and Discussion

Synthesis and Characterization

Mixing of $[Pt(PVM)_2(NH_3)_2]\cdot 2H_2O$[6] with $RhCl_3\cdot 3H_2O$ in MeOH provided a dinuclear Pt–Rh complex, $[PtRh(PVM)_2(NH_3)_2Cl_3]\cdot 4H_2O$ (**1**) (Scheme 3). The reaction was stoichiometrically complete within 3 d at 40 °C, where the solution color changed from dark red to dark brown. The dark brown MeOH solution was concentrated, and then excess KCl in H_2O was added to yield the pure product, which was confirmed by ^1H NMR spectroscopic analysis. The ^1H NMR spectra of **1** shows a single peak at δ = 1.19 ppm for the *t*Bu moieties,[8] which is apparently shifted from the peak at δ = 1.10 ppm for the *t*Bu moieties in $[Pt(PVM)_2(NH_3)_2]\cdot 2H_2O$.[6a] Figure 1a shows the ESI-MS (positive) spectra of **1** by dilution in MeOH. The peak at *m*/*z* = 1241, attributed to the dinuclear complex, was observed and the simulated isotope pattern based on the dinuclear complex apparently coincides with the observed one.

Other Pt–Rh dinuclear complexes with various amidates (TCM = Cl_3CCONH^-, BZM = $PhCONH^-$) and coligands, $[PtRh(PVM)_2(en)Cl_3]\cdot 3H_2O$ (**2**), $[PtRh(PVM)_2(NH_2CH_3)_2Cl_3]\cdot 3H_2O$ (**3**), $[PtRh(PVM)_2(NH_2tBu)_2Cl_3]\cdot 3H_2O$ (**4**), $[PtRh(TCM)_2(NH_3)_2Cl_3]$ (**5**), and $[PtRh(BZM)_2(NH_3)_2Cl_3]\cdot H_2O$ (**6**), were also obtained in a similar manner from the Pt mononuclear complexes having the noncoordinated oxygen atoms in the amide moieties; *cis*-$[Pt(PVM)_2(en)]\cdot 4H_2O$, *cis*-$[Pt(PVM)_2(NH_2CH_3)_2]\cdot H_2O$, *cis*-$[Pt(PVM)_2(NH_2tBu)_2]$, *cis*-$[Pt(TCM)_2(NH_3)_2]$, and *cis*-$[Pt(BZM)_2(NH_3)_2]$.[9] As shown in Figure 1, the ESI-MS peaks attributed to each dinuclear complex (**2**–**6**) were observed.

Crystal Structure of $[PtRh(PVM)_2(NH_3)_2Cl_3]\cdot 4H_2O$ (1)

Figure 2 shows the crystal structure of **1**, and Table 1 summarizes the selected bond lengths and angles for **1**. The single-crystal consists of Pt and Rh dinuclear complexes in which the two metal ions are doubly bridged by two PVM

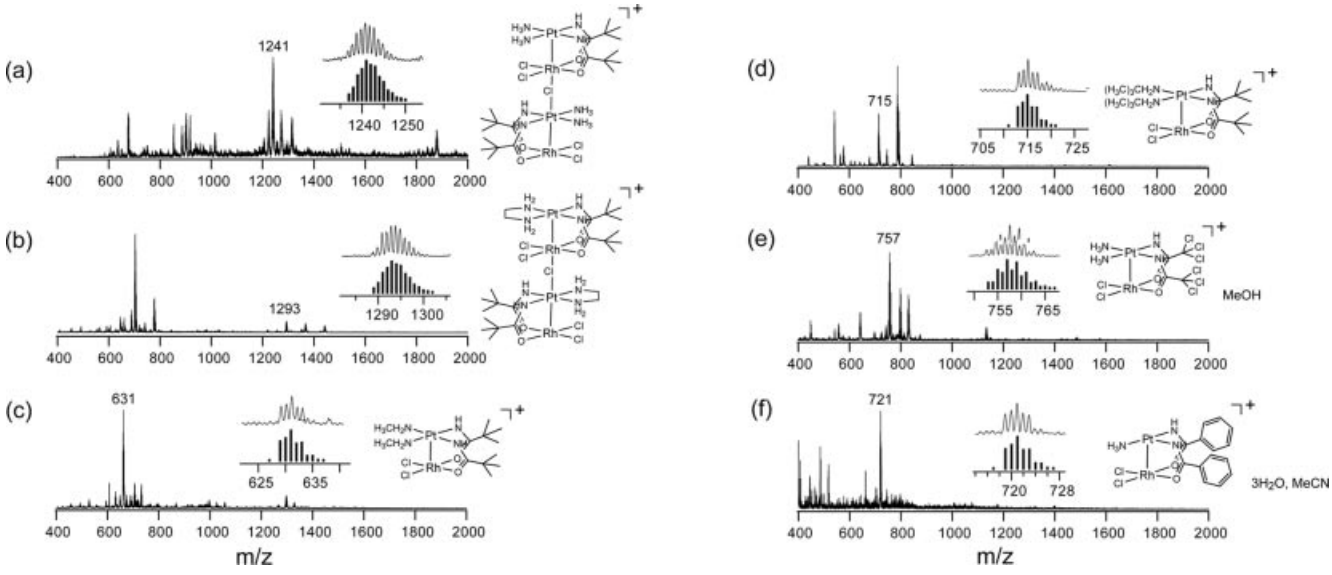

Figure 1. ESI-MS (positive) spectra for (a) **1**, (b) **2**, (c) **3**, (d) **4**, (e) **5**, and (f) **6**. Complexes **1**–**5** and **6** were measured by dilution in MeOH and MeOH/MeCN (v/v = 1:1), respectively.

ligands (Figure 2a). The asymmetric unit consists of Pt(1), Rh(1), Cl(1–3), one amine [N(1)], and one PVM [including O(1), O(2), N(2), and C(1)] ligand, with a crystallographic mirror along the *ab* plane [along the Pt(1)–Rh(1)–Cl(1) line]. The *cis* coordinated Cl(2)/Cl(3) and O(1)/O(2) atoms are in a disordered relationship with the 0.50/0.50 occupancy level, which means that two kinds of Rh(1) coordination planes, O(2)–O(1′)–Cl(2′)–Cl(3) and O(1)–O(2′)–Cl(3′)–Cl(2), are present in the crystal with a 50:50 ratio.

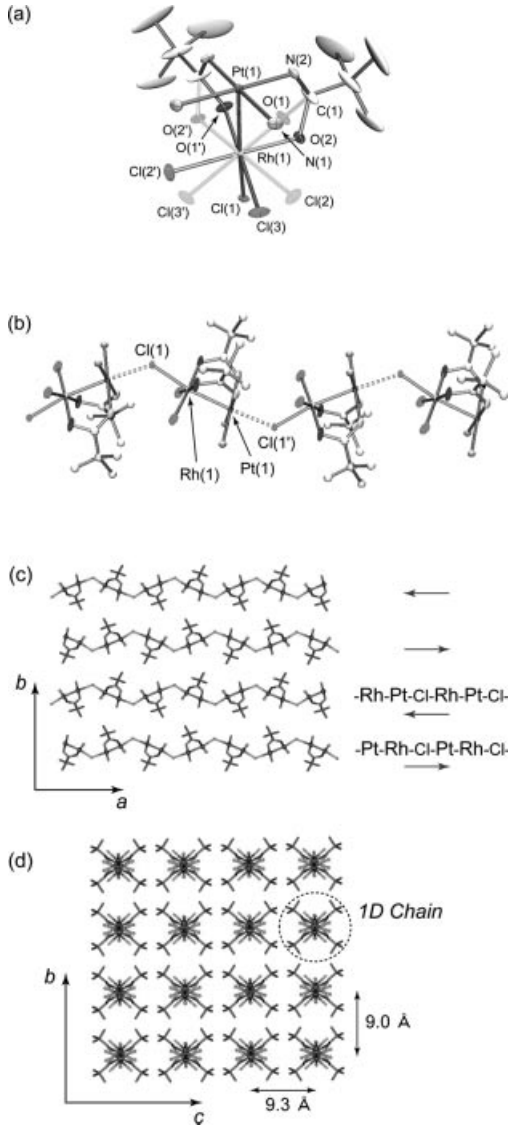

Figure 2. Crystal structure of $[PtRh(PVM)_2(NH_3)_2Cl_3]\cdot 4H_2O$ (**1**). (a) ORTEP drawing of **1** at the 30% probability level. Hydrogen atoms and water molecules are omitted for clarity. O(1) and O(2), and Cl(2) and Cl(3) atoms are in a disordered relationship. (b) Pseudo 1D chain where axially coordinated Cl(1) atoms bridge the dinuclear complexes. (c) Four pseudo 1D chains are aligned in parallel. Arrows indicate the chain directions. (d) Crystal packing diagram along the *a* axis. Water molecules are omitted for clarity.

Within the dimer, the Pt and Rh atoms are separated by 2.5704(7) Å (**1**). The Pt atom is *cis* coordinated with two amine ligands and two deprotonated nitrogen atoms of the PVM ligands. The Rh atom is coordinated by three Cl^- ions, two *cis* in the equatorial plane and one axially coordinated to Rh with the distances Rh(1)–Cl(1) = 2.4127(18), Rh(1)–Cl(2) = 2.333(3), and Rh(1)–Cl(3) = 2.329(3) Å. The coordination planes of the two metals are slightly tilted by 11.9°.

Table 1. Selected distances [Å] and angles [°] for $[PtRh(PVM)_2(NH_3)_2Cl_3]\cdot 4H_2O$ (**1**).[a]

Bond lengths			
Pt(1)–Rh(1)	2.5704(7)	Pt(1)–Cl(1)[1]	2.6328(17)
Pt(1)–N(1)	2.078(5)	Pt(1)–N(2)	1.995(5)
Rh(1)–Cl(1)	2.4127(18)	Rh(1)–Cl(2)	2.333(3)
Rh(1)–Cl(3)	2.329(3)	Rh(1)–O(1)	2.039(8)
Rh(1)–O(2)	2.026(9)	C(1)–N(2)	1.276(9)
C(1)–O(1)	1.372(12)	C(1)–O(2)	1.358(11)
Bond angles			
N(2)–Pt(1)–N(1)	88.5(2)	N(2)[2]–Pt(1)–N(2)	90.6(3)
N(2)–C(1)–O(1)	115.8(7)	N(2)–C(1)–O(2)	118.5(7)
Rh(1)–Pt(1)–Cl(1)[1]	176.92(4)	Cl(1)–Rh(1)–Pt(1)	171.08(5)
Rh(1)–Cl(1)–Pt(1)[3]	127.42(7)		

[a] Symmetry operators: (1) $x-1/2, -y+1/2, z$; (2) $x, y, -z$; (3) $x+1/2, -y+1/2, z$.

As shown in Figure 2b, the axially coordinated Cl^- ion on the Rh atom contacts the neighboring Pt atom with a distance of 2.6328(17) Å and bridges two Pt–Rh dimers. As to the packing of the Pt–Rh dimers, infinite strands of the head–head dimers are formed to give chains with the expression $[–Pt–Rh–Cl–]_n$. All chains run along the *a* axis, where adjacent chains run in the opposite direction as shown in Figure 2c. The one-dimensional chains are not linear but zigzag; the bridging Cl^- ions form the zigzag chains with the angle Rh(1)–Cl(1)–Pt(1′) = 127.42(7)°. All the chains run along the *a* axis without significant interaction between them (Figure 2d); the distances between the chain centers are about 9.0 and 9.3 Å.

Crystal Structure of $[PtRh(PVM)_2(en)Cl_3]\cdot 3H_2O$ (2)

Figure 3 shows the crystal structure of **2**, and Table 2 summarizes the selected bond lengths and angles for **2**. Compound **2** contains two individual dinuclear complexes in the unit cell. The asymmetric unit consists of Cl(1), Rh(1), Pt(1), Cl(3), Rh(2), Pt(2), two amines, and two PVM ligands, with a crystallographic mirror along the *ac* plane [along the Cl(1)–Rh(1)–Pt(1)–Cl(3)–Rh(2)–Pt(2) line] (Figure 3a). The carbon atoms C(1)/C(2) and C(8)/C(9) in the en ligands are disordered with the 0.58/0.42 occupancy level. Similar to **1**, the Pt and Rh ions in the dinuclear complexes are doubly bridged by two PVM ligands. The Pt atom is *cis* coordinated by four N-donor ligands; one en and two PVM ligands. The Rh atom is coordinated by three Cl^- ions, of which the axially coordinated Cl^- ion bridges two Pt–Rh dimers (Figure 3b). The distances between Pt and Rh are 2.5796(19) and 2.5771(17) Å. The coordination planes of the two metals are slightly tilted by 11.8 and 13.8°.

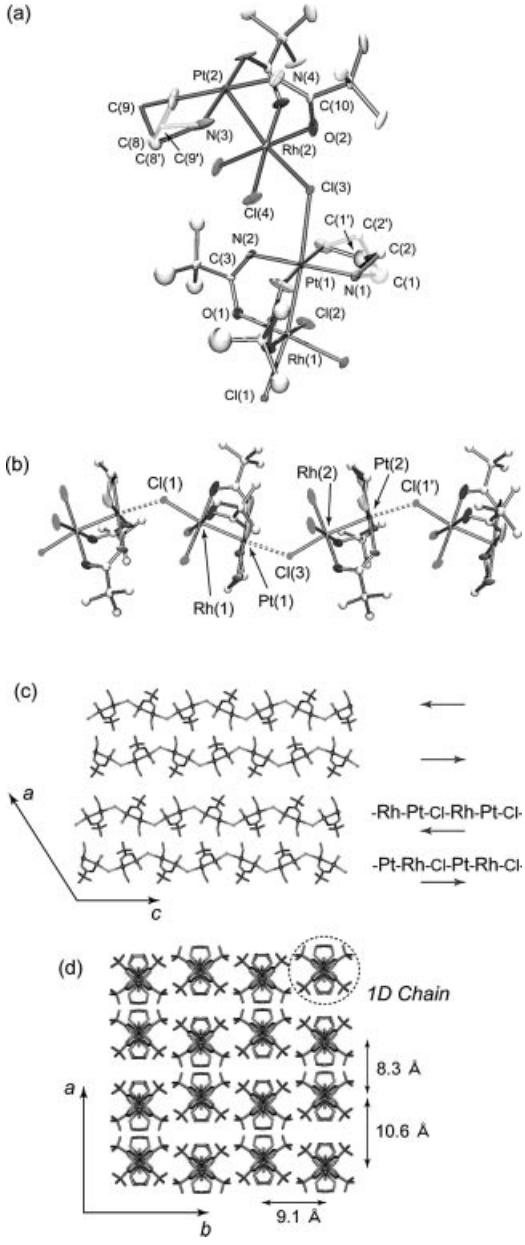

Figure 3. Crystal structure of $[PtRh(PVM)_2(en)Cl_3]\cdot 3H_2O$ (**2**). (a) ORTEP drawing of **2** at the 30% probability level. Hydrogen atoms and water molecules are omitted for clarity. C(1) and C(2), and C(8) and C(9) atoms are in a disordered relationship. (b) Pseudo 1D chain where axially coordinated Cl(1) and Cl (3) atoms bridge the dinuclear complexes. (c) Four pseudo 1D chains are aligned in parallel. Arrows indicate the chain directions. (d) Crystal packing diagram along the *c* axis. Water molecules are omitted for clarity.

As found in the packing structure of **2** (Figure 3c and Figure 3d), the pseudo 1D chain consists of the repetition of head–head dimers with the expression $[–Pt–Rh–Cl–]_n$, in a similar manner to **1**. The one-dimensional chains of **2** also zigzag, where the $Cl^–$ ions form bent bridges between the dimers with the angles of 128.08(18) and 129.26(19)°. The distances between Pt and axially contacted Cl atoms [Pt(1)···Cl(3) = 2.662(5), Pt(2)···Cl(1′) = 2.692(4) Å] in **2** are slightly longer than the corresponding one in **1**: Pt(1)···Cl(1′) = 2.6328(17) Å. As shown in Figure 3d, two

Table 2. Selected distances [Å] and angles [°] for $[PtRh(PVM)_2(en)Cl_3]\cdot 3H_2O$ (**2**).[a]

Bond lengths			
Pt(1)–Rh(1)	2.5796(19)	Pt(2)–Rh(2)	2.5771(17)
Pt(1)–Cl(3)	2.662(5)	Pt(2)–Cl(1)[1]	2.692(4)
Pt(1)–N(1)	2.058(13)	Pt(1)–N(2)	1.977(13)
Pt(2)–N(3)	2.055(14)	Pt(2)–N(4)	1.988(13)
Rh(1)–Cl(1)	2.410(4)	Rh(1)–Cl(2)	2.328(4)
Rh(2)–Cl(3)	2.420(5)	Rh(2)–Cl(4)	2.308(4)
Rh(1)–O(1)	2.033(10)	Rh(2)–O(2)	2.022(10)
C(3)–N(2)	1.266(19)	C(3)–O(1)	1.252(15)
C(10)–N(4)	1.264(18)	C(10)–O(2)	1.265(16)
Bond angles			
N(2)–Pt(1)–N(1)	90.5(8)	N(2)–Pt(1)–N(2)[2]	93.1(13)
N(4)–Pt(2)–N(3)	91.6(9)	N(4)[2]–Pt(2)–N(4)	89.9(11)
O(1)–Rh(1)–Cl(2)	86.7(3)	O(1)–Rh(1)–O(1)[2]	92.7(6)
O(2)–Rh(2)–Cl(4)	90.5(5)	O(2)[2]–Rh(2)–O(2)	87.3(8)
N(2)–C(3)–O(1)	121.6(14)	N(4)–C(10)–O(2)	121.9(13)
Rh(1)–Pt(1)–Cl(3)	174.81(10)	Rh(2)–Pt(2)–Cl(1)[1]	175.50(10)
Cl(1)–Rh(1)–Pt(1)	170.76(12)	Cl(3)–Rh(2)–Pt(2)	171.25(13)
Rh(1)–Cl(1)–Pt(2)[3]	128.08(18)	Rh(2)–Cl(3)–Pt(1)	129.26(19)

[a] Symmetry operators: (1) *x*, *y*, *z* + 1; (2) *x*, –*y* + 1, *z*; (3) *x*, *y*, *z*– 1.

parallel chains run in the opposite directions, $[–Pt–Rh–Cl–]_n$ and $[–Cl–Rh–Pt–]_n$, in close proximity of about 8.3 Å.

Both **1** and **2** give pseudo 1D infinite chains expressed as –MM′X–. A substantial number of halogen bridged chains have been thoroughly investigated to date, namely: (1) –MX– type chains,[5] (2) –MMX– type chains,[4] (3) the $Cl^–$-bridged platinum tan {= HH-$[Pt(2.5+)_4(NH_3)_8(\mu\text{-}C_4H_6NO)_4(Cl)]_n^{5n+}$, "platinum tan"[10] is the dark red amidate-bridged Pt tetranuclear complex containing the $Pt(2.5+)_4$ mixed valency} expressed as the M_4X-type chain.[11] In contrast, the present quasi 1D system is distinctly different from the previous systems on the ground that two kinds of metal ions are conjugated in the system (–MM′X– type chain).

Determination of the Oxidation States

The X-ray analysis of **1** and **2** revealed that the three $Cl^–$ ions and two amidate ligands are coordinated in the dinuclear unit, which indicates that the total oxidation state of the Pt–Rh core is +5. Considering the general oxidation states of the Pt and Rh atoms, possible formal oxidation states of **1** and **2** are Pt(+3)–Rh(+2) and Pt(+2)–Rh(+3). In order to determine the oxidation state of the metal ions in the Pt–Rh dinuclear complexes, XPS and ^{195}Pt NMR measurements were carried out.

Figure 4 shows the Rh $3d_{5/2}$ and $3d_{3/2}$, and Pt $4f_{7/2}$ and $4f_{5/2}$ core level spectra for **1**–**6** at room temperature. In the $3d_{3/2}$ region of rhodium, Pt $4d_{5/2}$ signals also exist but are overlapped with the Rh signals. The Pt $4f_{7/2}$ binding energies were determined as 73.4 (**1**) and 73.3 (**2**), which are closer to that of the Pt(+2) complex $[Pt^{II}(en)_2(\alpha\text{-pyridonato})_2](NO_3)_2$ (72.6 eV) than that of the Pt(+3) complex $[Pt^{III}(NH_3)_4(\alpha\text{-pyrrolidonato})_2(NO_3)_2](NO_3)_2$ (75.0 eV).[12] On the other hand, the Rh $3d_{5/2}$ binding energies obtained

are 309.4 (**1**) and 309.2 (**2**), which are close to the value of Rh(+3) in $RhCl_3 \cdot 3H_2O$ (310.0 eV).[13] As shown in Table 3, compounds **3**–**6** have binding energies similar to those of **1** and **2**.

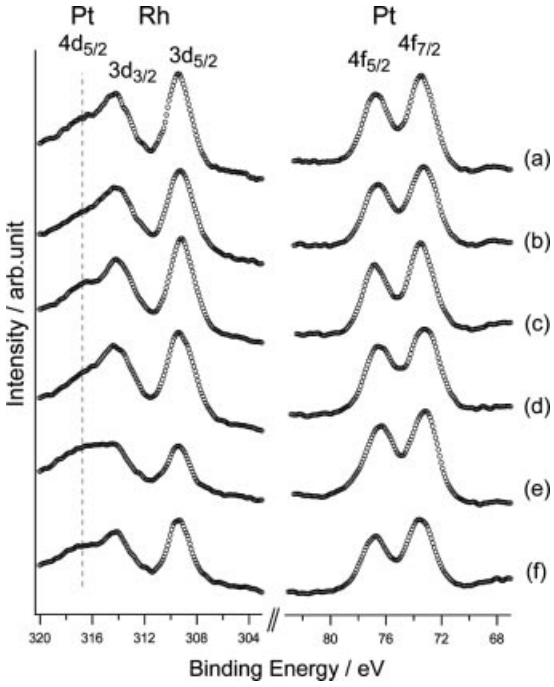

Figure 4. Rh $3d_{5/2}$ and $3d_{3/2}$ (left), Pt $4f_{7/2}$ and $4f_{5/2}$ (right) core levels of XPS for (a) **1**, (b) **2**, (c) **3**, (d) **4**, (e) **5**, and (f) **6**.

Table 3. Binding energy (eV) for 3d region of rhodium and 4f region of platinum in **1**–**6**.

Complex	Rh $3d_{3/2}$	Rh $3d_{5/2}$	Pt $4f_{5/2}$	Pt $4f_{7/2}$
1	314.2	309.4	76.7	73.4
2	314.1	309.2	76.5	73.3
3	314.2	309.1	76.8	73.5
4	314.4	309.4	76.6	73.2
5	314.2	309.4	76.3	73.1
6	314.1	309.3	76.7	73.6

Furthermore, the ^{195}Pt NMR chemical shifts obtained in MeOD by using an aqueous solution of $K_2[PtCl_6]$ as the external reference are –2452 (**1**), –2590 (**2**), –2365 (**3**), –2642 (**4**), and –2371 ppm (**5**), which are in the expected range for Pt(+2) complexes.[14,15] The broad line widths of the ^{195}Pt NMR signals are probably due to the interactions with ^{14}N nuclear spins. Compounds **4** and **5** did not show well-defined ^{195}Pt NMR signals in MeOD because of equilibrium mixing.[15] Interestingly, the ^{195}Pt chemical shifts for **1**–**5** are dispersed in a rather wide range (–2365 to –2642 ppm), which shows that there is a significant difference in the electronic states among them. Considering the results of XPS and ^{195}Pt NMR, we conclude that the formal oxidation state of the metal ions in **1**–**6** is Pt(+2, d^8)···Rh(+3, d^6).

Comparison with Other Pt–Rh Dinuclear Complexes

Previously, we reported unique heterometal chains with mixed valence (so-called HMMs), $\{[PtRh(PVM)_2(NH_3)_2Cl_{2.5}]_2[Pt_2(PVM)_2(NH_3)_4]_2(PF_6)_6 \cdot 2MeOH \cdot 2H_2O\}_n$ (HMM-**1**), that comprised Pt–Rh and Pt–Pt dinuclear complexes possessing an unpaired electron over the octanuclear unit.[16] Compound **1** corresponds to a fragment of the octanuclear repetition unit in HMM-**1**. Because the HOMO is in the Pt–Rh dinuclear metal orbital part in HMM-**1**,[16] comparison between **1** and HMM-**1** is meaningful. As shown in Table 4, the Pt–Rh distances in **1** and **2** are slightly shorter than that of Pt(+3, d^7)···Rh(+2.5, $d^{6.5}$) in HMM-**1**.[16]

Table 4. Pt–Rh oxidation states and distances [Å].

Compound	Oxidation states	Pt–Rh distance	Ref.
[a]	Pt(+2, d^8)···Rh(+1, d^8)	3.043(1)	[17]
[b]	Pt(+2, d^8)···Rh(+1, d^8)	3.079(2)	[18]
HMM-**1**	Pt(+3, d^7)···Rh(+2.5, $d^{6.5}$)	2.5987(11)	[19]
1	Pt(+2, d^8)···Rh(+3, d^6)	2.5704(7)	this work
2	Pt(+2, d^8)···Rh(+3, d^6)	2.5796(19)	this work

[a] = *trans*-Rh–(CO)Cl(μ-$Ph_2AsCH_2PPh_2)_2$-*cis*-$PtCl_2$. [b] = $[(NC)_2PtRh(CNtBu)_2(\mu\text{-dpm})_2](PF_6)$ [μ-dpm = bis(diphenylphosphanyl)methane].

In addition, the Pt–Rh distances in **1** and **2** are about 0.5 Å shorter than those reported in other Pt–Rh dinuclear complexes, *trans*-Rh–(CO)Cl(μ-$Ph_2AsCH_2PPh_2)_2$-*cis*-$PtCl_2$ (***a***)[17] and $[(NC)_2PtRh(CNtBu)_2(\mu\text{-dpm})_2](PF_6)$ (***b***, μ-dpm = bis(diphenylphosphanyl)methane),[18] where the formal oxidation states are Pt(+2, d^8)···Rh(+1, d^8). It has been shown that an occupied d_{z^2} orbital in the d^8 transition metal ion with square-planar coordination geometry can act as a donor to other metal ions (M′) to form a dative Pt(d^8)→M′ bond.[19] Considering the short Pt–Rh distances, compounds **1** and **2** are considered to have a dative Pt(d^8)→Rh(d^6) bond, where the Pt d_{z^2} orbital is stabilized by the overlap with the d_{z^2} orbital of Rh.

Conclusions

The present study is focused on the synthesis and single-crystal X-ray analysis of novel Pt–Rh dinuclear complexes having a Pt–Rh bond doubly bridged by amidate ligands, and we have succeeded in obtaining six dinuclear complexes with various amidate and amine ligands. Compounds **1** and **2** are zigzag MM′X chains, and XPS and ^{195}Pt NMR spectroscopic measurements revealed that the dinuclear complexes have the formal oxidation state of Pt(+2, d^8)···Rh(+3, d^6). Apparently, there is no electronic interaction between the Pt–Rh dinuclear complex units bridged by Cl^- ions in the zigzag chain. Because linear 1D chains constructed from Pt and a heterometal are expected to have unique physical properties, attempts to straighten the alignment of the Pt–Rh dinuclear complexes in the chain by modifying the axial ligand is currently in progress.

Experimental Section

Synthesis of $[PtRh(PVM)_2(NH_3)_2Cl_3] \cdot 4H_2O$ (1): A MeOH solution (200 mL) of $[Pt(PVM)_2(NH_3)_2] \cdot 2H_2O$ (1 mmol, 0.47 g) was stirred

with $RhCl_3 \cdot 3H_2O$ (1 mmol, 0.26 g) for 3 d at 40 °C. The resulting brown solution was concentrated to yield a brown solid. The brown solid was stirred with an aqueous solution (10 mL) of KCl (4.0 mmol, 0.30 g) to give the brown product. Yield: 0.28 g (39%). The product was recrystallized by diffusing excess KCl into the aqueous solution to give suitable single crystals. IR (KBr pellet): C=O stretching, $\tilde{\nu}$ = 1639 (m), 1574 (s) cm^{-1}. $C_{10}H_{34}Cl_3N_4O_6PtRh$ (711): calcd. C 16.90, H 4.82, N 7.88; found C 17.12, H 4.51, N 7.09.

Synthesis of $[PtRh(PVM)_2(en)Cl_3] \cdot 3H_2O$ (2): A MeOH solution (300 mL) of $[Pt(PVM)_2(en)] \cdot 4H_2O$ (1.5 mmol, 0.79 g) was stirred with $RhCl_3 \cdot 3H_2O$ (1.5 mmol, 0.395 g) for 2 d at 40 °C. The resulting brown solution was concentrated to yield a brown solid. The brown solid was stirred with an aqueous solution (10 mL) of KCl (4.0 mmol, 0.30 g) to give the dark green product. Yield: 0.29 g (27%). The product was recrystallized by diffusing excess KCl into the aqueous solution to give suitable single crystals. IR (KBr pellet): C=O stretching, $\tilde{\nu}$ = 1635 (m), 1574 (s) cm^{-1}. $C_{12}H_{34}Cl_3N_4O_5PtRh$ (719): calcd. C 20.05, H 4.77, N 7.79; found C 20.30, H 4.43, N 7.64.

Synthesis of $[PtRh(PVM)_2(NH_2CH_3)_2Cl_3] \cdot 3H_2O$ (3): A MeOH solution (136 mL) of $[Pt(PVM)_2(NH_2CH_3)_2] \cdot H_2O$ (0.68 mmol, 0.32 g) was stirred with $RhCl_3 \cdot 3H_2O$ (0.68 mmol, 0.18 g) for 2 d at 40 °C. The resulting dark violet solution was concentrated to yield a dark violet solid. The dark violet solid was stirred with an aqueous solution (6.5 mL) of KCl (6.7 mmol, 0.50 g) to give the brown product. Yield: 0.15 g (31%). IR (KBr pellet): C=O stretching, $\tilde{\nu}$ = 1645 (m), 1570 (s) cm^{-1}. $C_{12}H_{36}Cl_3N_4O_5PtRh$ (721): calcd. C 20.00, H 5.03, N 7.77; found C 20.40, H 4.50, N, 7.17.

Synthesis of $[PtRh(PVM)_2(NH_2tBu)_2Cl_3] \cdot 3H_2O$ (4): A MeOH solution (90 mL) of $[Pt(PVM)_2(NH_2tBu)_2]$ (0.45 mmol, 0.24 g) was stirred with $RhCl_3 \cdot 3H_2O$ (0.45 mmol, 0.12 g) for 2 d at 40 °C. The resulting brown solution was concentrated to yield a brown solid. The brown solid was stirred with an aqueous solution (5 mL) of KCl (1.3 mmol, 0.10 g) to give the brown product. Yield: 0.23 g (63%). IR (KBr pellet): C=O stretching, $\tilde{\nu}$ = 1647 (m), 1571 (s) cm^{-1}. $C_{18}H_{48}Cl_3N_4O_5PtRh$ (805): calcd. C 26.86, H 6.01, N, 6.96; found C 25.90, H 5.16, N 6.01.

Synthesis of $[PtRh(TCM)_2(NH_3)_2Cl_3]$ (5): A MeOH solution (150 mL) of $[Pt(TCM)_2(NH_3)_2]$ (0.75 mmol, 0.41 g) was stirred with $RhCl_3 \cdot 3H_2O$ (0.75 mmol, 0.20 g) for 3 d at 40 °C. The resulting brown solution was concentrated to yield a brown solid. The brown solid was stirred with an aqueous solution (4 mL) of NaCl (10.3 mmol, 0.60 g) to give the dark green product. Yield: 0.25 g (43%). IR (KBr pellet): C=O stretching, $\tilde{\nu}$ = 1716 (m), 1628 (s) cm^{-1}. $C_4H_8Cl_9N_4O_2PtRh$ (761): calcd. C 6.31, H 1.06, N, 7.36; found C 6.31, H 1.50, N 7.33.

Synthesis of $[PtRh(BZM)_2(NH_3)_2Cl_3] \cdot H_2O$ (6): A MeOH solution (120 mL) of $[Pt(BZM)_2(NH_3)_2]$ (0.6 mmol, 0.28 g) was stirred with $RhCl_3 \cdot 3H_2O$ (0.6 mmol, 0.16 g) for 3 d at 40 °C. The resulting brown solution was concentrated to yield a brown solid. The brown solid was stirred with an aqueous solution (4 mL) of KCl (9.3 mmol, 0.70 g) to give the brown product. Yield: 0.18 g (42%). IR (KBr pellet): C=O stretching, $\tilde{\nu}$ = 1597 (m), 1558 (s) cm^{-1}. $C_{14}H_{20}Cl_3N_4O_3PtRh$ (697): calcd. C 24.14, H 2.89, N 8.04; found C 24.38, H 2.91, N 7.48.

X-ray Structure Determination for 1 and 2: Measurements were carried out with a Bruker SMART APEX CCD diffractometer equipped with a normal focus Mo-target X-ray tube (λ = 0.71073 Å) operated at 2000 W power (50 kV, 40 mA) and a CCD two-dimensional detector. A total of 1315 frames were collected with a scan width of 0.3° in ω with an exposure time of 20 (**1**) and 40 (**2**) s/frame. The frames were integrated with the SAINT software package with a narrow frame algorithm.[20] Absorption correction was applied by using SADABS.[21] All the structures were solved by direct methods with the subsequent difference Fourier syntheses and the refinement with the SHELXTL (version 5.1) software package.[22] For all compounds, the non-hydrogen atoms were refined anisotropically and all hydrogen atoms were placed in the ideal positions. In **1**, O(1) and O(2), Cl(2) and Cl(3) atoms were refined with disorder relationship. In **2**, C(1) and C(2), C(8) and C(9) atoms were refined with disorder relationship. In **2**, C(1), C(2), C(5)–(9), O(4) and O(6) were isotropically refined under rigid conditions (Table 5). CCDC-618494 (for **1**) and -618495 (for **2**) contain the supplementary crystallographic data for this paper. These data can be obtained free of charge from The Cambridge Crystallographic Data Centre via www.ccdc.cam.ac.uk/data_request/cif.

Table 5. Crystal data and structure refinement for $[PtRh(PVM)_2(NH_3)_2Cl_3] \cdot 4H_2O$ (**1**) and $[PtRh(PVM)_2(en)Cl_3] \cdot 3H_2O$ (**2**).

Compound	**1**	**2**
Formula	$C_{10}H_{20}Cl_3N_4O_6PtRh$	$C_{12}H_{20}Cl_3N_4O_5PtRh$
Formula mass	696.65	704.67
Crystal system	orthorhombic	monoclinic
Space group	*Ibam* (no. 72)	*C2/m* (no. 12)
a [Å]	13.7371(17)	22.050(10)
b [Å]	18.002(2)	18.260(8)
c [Å]	18.541(2)	13.865(6)
α [°]	90	90
β [°]	90	122.138(7)
γ [°]	90	90
V [Å^3]	4585.1(10)	4727(4)
Z	8	8
$D_{calcd.}$ [g cm^{-3}]	2.018	1.980
μ [mm^{-1}]	7.193	6.975
R_1[a] [$I > 2.0\sigma(I)$]	0.0266	0.0710
wR_2[b] [all data]	0.1034	0.2001
T [°C]	–153	–153

[a] $R_1 = \Sigma(|F_o| - |F_c|)/\Sigma(|F_o|)$. [b] $wR_2 = \{\Sigma[w(F_o^2 - F_c^2)^2]/\Sigma[w(F_o^2)^2]\}^{1/2}$.

Physical Measurements: The X-ray photoelectron spectroscopy measurements were carried out with a JEOL JPS-9010. Binding energies were measured relative to the C 1s peak (284.8 eV) of internal hydrocarbon.

Supporting Information (see footnote on the first page of this article): ^{1}H NMR spectra for **1**–**4**, IR spectra for **1**–**6**, ^{195}Pt NMR spectra for **1**–**5**.

Acknowledgments

This work was supported by Iketani Science and Technology Foundation, Grants-in-Aid for Scientific Research [Young Scientist (B) No. 17750058], and the 21COE program "Practical Nano-Chemistry" from MEXT, Japan.

[1] a) J. S. Miller, *Extended Linear Chain Compounds, Vols. 1–3*, Plenum, New York, **1982**.; b) J. K. Bera, K. R. Dunbar, *Angew. Chem. Int. Ed.* **2002**, *41*, 4453–4457.

[2] a) K. Sakai, M. Takeshita, Y. Tanaka, T. Ue, M. Yanagisawa, M. Kosaka, T. Tsubomura, M. Ato, T. Nakano, *J. Am. Chem. Soc.* **1998**, *120*, 11353–11363; b) K. Sakai, E. Ishigami, Y. Konno, T. Kajiwara, T. Ito, *J. Am. Chem. Soc.* **2002**, *124*, 12088–12089; c) M. Yamashita, D. Kawakami, S. Matsunaga, Y. Nakayama, M. Sasaki, S. Takaishi, F. Iwahori, H. Miyasaka, K. Sugiura, Y. Wada, H. Miyamae, H. Matsuzaki, H.

Okamoto, H. Tanaka, K. Marumoto, S. Kuroda, *Angew. Chem. Int. Ed.* **2004**, *43*, 4763–4767.
[3] a) G. M. Finniss, E. Canadell, C. Campana, K. R. Dunbar, *Angew. Chem. Int. Ed. Engl.* **1996**, *35*, 2772–2774; b) M. E. Prater, L. E. Pence, R. Clerac, G. M. Finniss, C. Campana, P. Auban-Senzier, D. Jerome, E. Canadell, K. R. Dunbar, *J. Am. Chem. Soc.* **1999**, *121*, 8005–8016; c) F. A. Cotton, E. V. Dikarev, M. A. Petrukhina, *J. Organomet. Chem.* **2000**, *596*, 130–135; d) F. A. Cotton, E. V. Dikarev, M. A. Petrukhina, *J. Chem. Soc., Dalton Trans.* **2000**, 4241–4243; e) F. P. Pruchnik, P. Jakimowicz, Z. Ciunik, *Inorg. Chem. Commun.* **2001**, *4*, 726–729; f) M. Mitsumi, S. Umebayashi, Y. Ozawa, M. Tadokoro, H. Kawamura, K. Toriumi, *Chem. Lett.* **2004**, *33*, 970–971; g) M. Mitsumi, H. Goto, S. Umebayashi, Y. Ozawa, M. Kobayashi, T. Yokoyama, H. Tanaka, S.-i. Kuroda, K. Toriumi, *Angew. Chem. Int. Ed.* **2005**, *44*, 4164–4168.
[4] a) H. Kitagawa, N. Onodera, T. Sonoyama, M. Yamamoto, T. Fukawa, T. Mitani, M. Seto, Y. Maeda, *J. Am. Chem. Soc.* **1999**, *121*, 10068–10080; b) H. Kitagawa, T. Mitani, *Coord. Chem. Rev.* **1999**, *190–192*, 1169–1184; c) M. Mitsumi, T. Murase, H. Kishida, T. Yoshinari, Y. Ozawa, K. Toriumi, T. Sonoyama, H. Kitagawa, T. Mitani, *J. Am. Chem. Soc.* **2001**, *123*, 11179–11192.
[5] M. Yamashita, D. Kawakami, S. Matsunaga, Y. Nakayama, M. Sasaki, S. Takaishi, F. Iwahori, H. Miyasaka, K. Sugiura, Y. Wada, H. Miyamae, H. Matsuzaki, H. Okamoto, H. Tanaka, K. Marumoto, S. Kuroda, *Angew. Chem. Int. Ed.* **2004**, *43*, 4763.
[6] a) W. Chen, K. Matsumoto, *Inorg. Chim. Acta* **2003**, *342*, 88–96; b) W. Chen, F. Liu, T. Nishioka, K. Matsumoto, *Eur. J. Inorg. Chem.* **2003**, 4234–4243.
[7] a) A. Erxleben, I. Mutikainen, B. Lippert, *J. Chem. Soc., Dalton Trans.* **1994**, 3667–3675; b) E. Zangrando, F. Pichierri, L. Randaccio, B. Lippert, *Coord. Chem. Rev.* **1996**, *156*, 275–332.
[8] The ^{1}H NMR spectrum is shown in the Supporting Information.
[9] K. Uemura, K. Yamasaki, K. Fukui, K. Matsumoto, unpublished work; Similarly to the previous procedure,[6a] five new mononuclear platinum complexes with noncoordinated oxygen atoms in the amide ligands were successfully obtained.
[10] K. Matsumoto, K. Fuwa, *J. Am. Chem. Soc.* **1982**, *104*, 897–898.
[11] K. Sakai, Y. Tanaka, Y. Tsuchiya, K. Hirata, T. Tsubomura, S. Iijima, A. Bhattacharjee, *J. Am. Chem. Soc.* **1998**, *120*, 8366–8379.
[12] K. Matsumoto, K. Sakai, K. Nishio, Y. Tokisue, R. Ito, T. Nishide, Y. Shichi, *J. Am. Chem. Soc.* **1992**, *114*, 8110–8118.
[13] C. Furlani, G. Mattogno, G. Polzonetti, G. Braca, G. Valentini, *Inorg. Chim. Acta* **1983**, *69*, 199–205.
[14] P. S. Pregosin, *Coord. Chem. Rev.* **1982**, *44*, 247–291.
[15] ^{195}Pt NMR spectra are shown in the Supporting Information. Compounds **4** and **5** (asterisk) did not show well-defined ^{195}Pt NMR signals in MeOD because of equilibrium mixing and the limited solubility. It seems that dissociation and coordination of the axial Cl^{-} ion occurs in equilibrium, which induces two species, $[PtRh(Amid)_2(Am)_2Cl_2]^{+}$ and $[PtRh(Amid)_2(Am)_2Cl_3]$ (Amid = amidate, Am = amine). Low solubility of **6** precluded ^{195}Pt NMR measurements.
[16] a) K. Uemura, K. Fukui, H. Nishikawa, S. Arai, K. Matsumoto, H. Oshio, *Angew. Chem. Int. Ed.* **2005**, *44*, 5459–5464; b) K. Uemura, K. Fukui, K. Yamasaki, K. Matsumoto, *Sci. Technol. Adv. Mater.* **2006**, 461–467.
[17] a) R. R. Guimerans, F. E. Wood, A. L. Balch, *Inorg. Chem.* **1984**, *23*, 1307–1308; b) A. L. Balch, R. R. Guimerans, J. Linehan, F. E. Wood, *Inorg. Chem.* **1985**, *24*, 2021–2026.
[18] A. L. Balch, V. J. Catalan, *Inorg. Chem.* **1992**, *31*, 3934–3942.
[19] a) F. A. Cotton, L. R. Falvello, R. Uson, J. Fornies, M. Tomas, J. M. Casas, I. Ara, *Inorg. Chem.* **1987**, *26*, 1366–1370; b) T. Yamaguchi, F. Yamazaki, T. Ito, *J. Am. Chem. Soc.* **1999**, *121*, 7405–7406; c) T. Yamaguchi, F. Yamazaki, T. Ito, *J. Am. Chem. Soc.* **2001**, *123*, 743–744.
[20] *SMART & SAINT Software Package v. 5.625*, Siemens Energy & Automation, Inc., Analytical Instrumentation, Madison, WI, **2001**.
[21] G. M. Sheldrick, *SADABS, Software for Empirical Absorption Corrections*, University of Göttingen, Germany, **1996**.
[22] *SHELXTL Reference Manual v. 5.1: Bruker AXS*, Analytical X-ray Systems, Madison, WI, **1997**.

Received: September 26, 2006
Published Online: January 5, 2007

